catalysts

MDPI

Article

Enantiopure C_1-symmetric *N*-Heterocyclic Carbene Ligands from Desymmetrized *meso*-1,2-Diphenylethylenediamine: Application in Ruthenium-Catalyzed Olefin Metathesis

Veronica Paradiso [1], Sergio Menta [2], Marco Pierini [2], Giorgio Della Sala [1], Alessia Ciogli [2,*] and Fabia Grisi [1,*]

1 Dipartimento di Chimica e Biologia "Adolfo Zambelli", Università di Salerno, Via Giovanni Paolo II 132, I-84084 Fisciano, Salerno, Italy; vparadiso@unisa.it (V.P.); gdsala@unisa.it (G.D.S.)

2 Dipartimento di Chimica e Tecnologie del Farmaco, Sapienza Università di Roma, Piazzale A. Moro 5, 00185 Roma, Italy; sergio.menta@uniroma1.it (S.M.); marco.pierini@uniroma1.it (M.P.)

* Correspondence: alessia.ciogli@uniroma1.it (A.C.); fgrisi@unisa.it (F.G.); Tel.: +39-064-969-3310 (A.C.); +39-089-969-557 (F.G.)

Academic Editor: Federico Cisnetti

Received: 14 October 2016; Accepted: 9 November 2016; Published: 14 November 2016

Abstract: In order to design improved chiral ruthenium catalysts for asymmetric olefin metathesis, enantiomeric catalysts incorporating C_1-symmetric *N*-Heterocyclic carbenes (NHC) ligands with *syn*-related substituents on the backbone were synthesized starting from *meso*-1,2-diphenylethylenediamine. The absolute configuration of the enantiomers of the desymmetrized *meso* diamine was assigned by optical rotation analysis and in silico calculations, and was found to be maintained in their respective ruthenium catalysts by comparison of the relative electronic circular dichroism (ECD) spectra. The catalytic behaviour of the enantiomeric ruthenium complexes was investigated in model asymmetric metathesis transformations and compared to that of analogous complexes bearing C_1-symmetric NHC ligands with an *anti* backbone. Modest enantioselectivities were registered and different catalyst properties depending on the nature of stereochemical relationship of substituents on the backbone were observed.

Keywords: chiral *N*-Heterocyclic carbenes; ruthenium catalysts; asymmetric olefin metathesis; enantioselective chromatography; chiro-optical characterization

1. Introduction

In the last two decades, *N*-Heterocyclic carbenes (NHCs) have become indispensable tools in both transition-metal-based catalysis and organocatalysis. The design of NHCs with tailored steric and electronic properties has enabled rapid development of highly efficient metal catalysts in a wide variety of academically and industrially important processes [1–4]. Among them, asymmetric transformations mediated by metal catalysts bearing NHCs with chiral architectures have attracted increasing interest, and intensive research efforts have permitted the obtainment of highly stereoselective catalysts [5,6]. The employment of stable, easy-handling chiral NHC Ru-based catalysts has resulted in significant advancements in asymmetric olefin metathesis, a powerful methodology for carbon-carbon bond formation leading to enantioenriched molecules [7–11]. A number of highly enantioselective catalysts bearing C_2- and C_1-symmetric NHC ligands derived from chiral 1,2-diamines were reported by Grubbs [12–14] and Collins [15–18] (Figure 1). Ru-catalysts containing C_1-symmetric bidentate or backbone-monosubstituted NHC ligands were introduced by Hoveyda [19–22] and Blechert [23,24], respectively, and both these classes of catalysts provided high enantiomeric excesses in model asymmetric reactions.

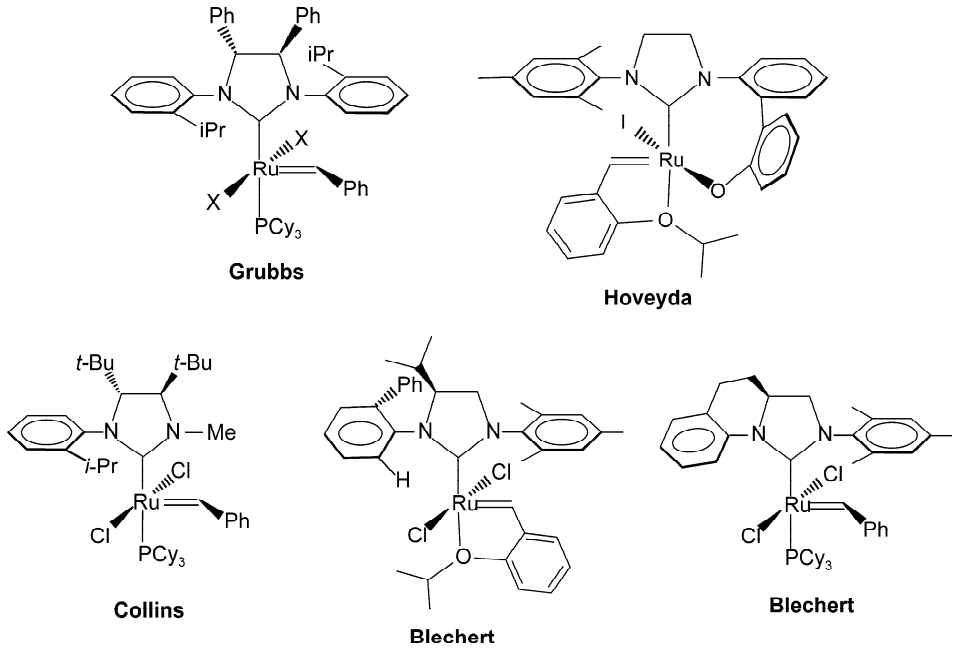

Figure 1. Selected examples of enantioselective ruthenium catalysts.

Recently, we reported chiral ruthenium catalysts **1**–**4** (Figure 2) bearing C_1-symmetric NHC ligands derived from (*R*,*R*)- and *meso*-1,2-diphenylehylenediamine. In representative olefin metathesis reactions (such as ring-closing metathesis, cross-metathesis, ring-opening metathesis polymerization), **1**–**4** displayed different catalytic efficiencies depending on the NHC backbone configuration (*anti* or *syn*) [25,26]. This finding intrigued us to investigate the effect of the different stereochemical relationship of substituents on the backbone in asymmetric metathesis transformations. Unfortunately, while catalysts **2** and **4** are enantiopure, **1** and **3** are obtained as racemic mixtures, and their resolution seems to be not trivial. As a consequence, we initially limited our investigation to enantiopure catalysts **2** and **4**, which were compared in model asymmetric ring-closing metathesis (ARCM) and asymmetric ring-opening cross-metathesis (AROCM), showing moderate enantioselectivity [26]. To overcome problems related to the resolution of racemic mixtures of catalysts with *syn* configuration, we thought to synthesize the latter in enantiopure form starting from the corresponding enantiomerically pure NHC ligands.

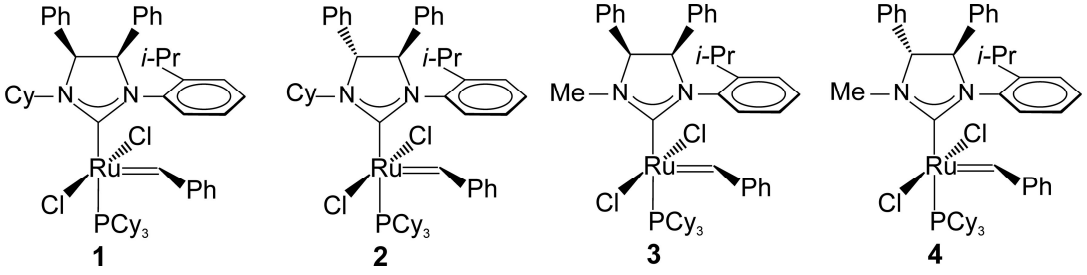

Figure 2. Ruthenium catalysts bearing C_1-symmetric *N*-Heterocyclic carbenes (NHCs) with different backbone configurations. **1** and **3** are racemic mixtures (only one of the enantiomers is depicted), **2** and **4** are enantiopure.

Therefore, herein we present for the first time the synthesis of enantiopure C_1-symmetric NHC precursors with *syn* phenyl groups on the backbone and *N*-cyclohexyl/*N*-2-isopropylphenyl substituents, achieved thanks to the successful desymmetrization of *meso*-1,2-diphenylethylenediamine

through derivatization followed by enantioselective chromatography. The assignment of the absolute configuration of the enantiomers of the desymmetrized *meso* molecule by optical rotation analysis and in silico calculations is also reported. The resulting enantiopure catalysts **1a** and **1b** are tested in model ARCM and AROCM reactions, and their catalytic behaviors are compared to those of catalysts **2** and **4** featuring an *anti* NHC backbone, providing an unprecedented evaluation of the impact of *syn* and *anti* backbone configuration of C_1-symmetric NHCs in asymmetric metathesis.

2. Results and Discussion

2.1. Synthesis of Catalyst 1a and 1b

The synthesis of enantiomerically pure catalysts **1a** and **1b** was carried out according to the synthetic route previously reported by us for the racemic complex **1** [25]. The required synthetic steps are illustrated in Scheme 1. Installation of a 2-isopropylphenyl group on one of the nitrogen atoms of *meso*-1,2-diphenylethylenediamine (**A**) through a Pd-catalyzed cross-coupling reaction resulted in a racemic mixture (**B**) which was separated in its constituent enantiomers by enantioselective high-performance liquid chromatography (HPLC). In order to ensure the purity of (+)-**B** and (−)-**B**, the enantiomeric excess (ee %) and the chiro-optical properties (namely optical rotatory dispersion, ORD and electronic circular dichroism, ECD) were determined for each collected enantiomer (see Section 2.2). Each enantiomer of **B** was condensed with cyclohexanone, and the resulting imine then reduced in situ with $NaBH_4$ to afford the corresponding enantiopure diamine (**C**). Reaction of each enantiomer of **C** with triethylorthoformate in the presence of $NaBF_4$ gave the corresponding enantiomerically pure NHC ligand precursor (**D**), which after deprotonation with potassium hexamethyldisilazide (KHMDS) and reaction with $RuCl_2(=CHPh)(PCy_3)_2$ (GI) provided respectively **1a** and **1b** in 42% and 47% yield respectively. Both the enantiomers were characterized by ^1H, ^{13}C and ^{31}P nuclear magnetic resonance (NMR) spectroscopy and ECD.

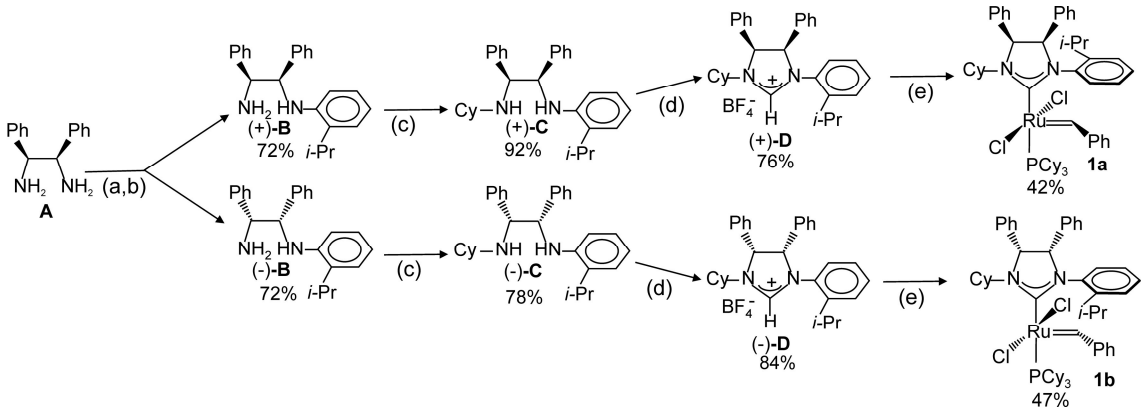

Scheme 1. Synthesis of **1a** and **1b**. (**a**) 2-isopropylphenylbromide, $Pd(acac)_2$, NaOtBu, (±)-2,2′-Bis (diphenylphosphino)-1,1′-binaphthalene (BINAP), toluene, 100 °C, 12 h, 90%; (**b**) enantioselective high-performance liquid chromatography (HPLC); (**c**) 1: cyclohexanone, CH_2Cl_2, RT, 12 h; 2: $NaBH_4$, CH_3OH, 4 h; (**d**) NH_4BF_4, $CH(OEt)_3$, 130 °C, 2 h; (**e**) potassium hexamethyldisilazide (KHMDS), GI, toluene, RT, 1 h.

Although it has not been possible to characterize the **1a** and **1b** catalysts by enantioselective HPLC, due to their instability in mobile phase conditions (in presence of alcohols), the off-line ECD spectrum of each enantiomer has been successfully recorded in hexane (Figure 3). In the spectral investigated window, ECD spectra showed Cotton effects at 212, 260, 290 and 350 nm: the first two bands present the same CD sign albeit opposite to the second two (i.e., 212/260 positive and 290/350 nm negative for **5a**) with a single null value (CD sign inversion point) at 280 nm.

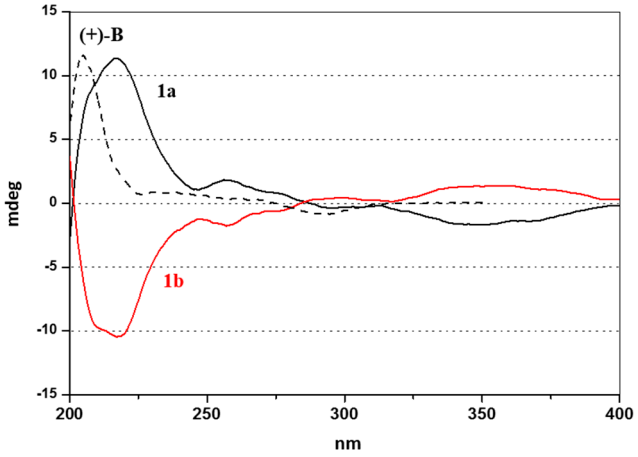

Figure 3. Electronic circular dichroism (ECD) spectra for the enantiopure **1a** and **1b** catalysts. Dotted trace refers to the ECD spectrum of (+)-**B**.

2.2. Enantioselective Chromatography and Chiro-Optical Characterization

The enantiomers of **B** were well resolved by enantioselective HPLC on the polysaccharide-based Chiralpak IA column under normal phase conditions with both UV and CD detections (k_1: 1.24, α: 1.50, T: 25 °C). Peaks in enantiomeric relationship are the third and fourth in the chromatographic UV profile of crude sample as confirmed by the opposite signal of CD trace (Figure 4a). Scaling up to semi-preparative conditions was straightforward. The α value gave access to high levels of enantiomeric purity and the short retention time (10 min) made this step not very time consuming for the whole process of synthesis and evaluation of enantiopure catalyst. However, the low solubility of the sample in the elution conditions did not allow us to take advantage of the high loading capacity of the stationary phase. A concentration of 50 mg/mL of starting sample was optimized to avoid precipitation, and finally 105 mg of each enantiomer were purified with enantiomeric excess for the first and second eluted enantiomer of 99.9% and 98.8%, respectively (Figure 4b,c).

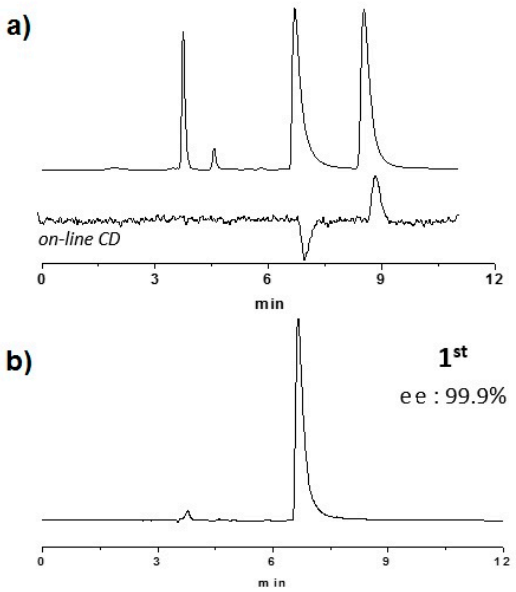

Figure 4. *Cont.*

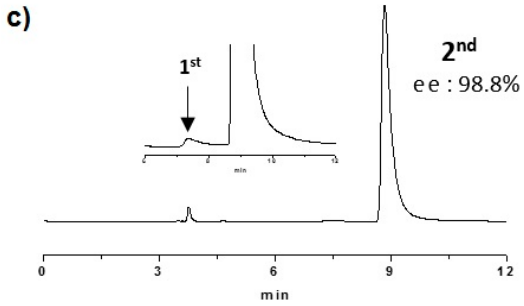

Figure 4. Analytical chromatographic profiles of crude sample (top UV and CD), analytical purity control of purified enantiomers (first eluted in (**a**) and second eluted in (**b**)). Experimental details in the text.

The off-line ECD spectra, recorded in 200–350 nm range, showed the typical mirror-image profile of pure samples in enantiomeric relationship (Figure 5a). In addition to complete the chiro-optical characterization, specific rotation measurements allowed to $[\alpha_D]^{20} = +172.5°$ for first and $[\alpha_D]^{20} = -171.1°$ for second eluted while the OR values were recorded at different wavelengths (Figure 5b and Table 1).

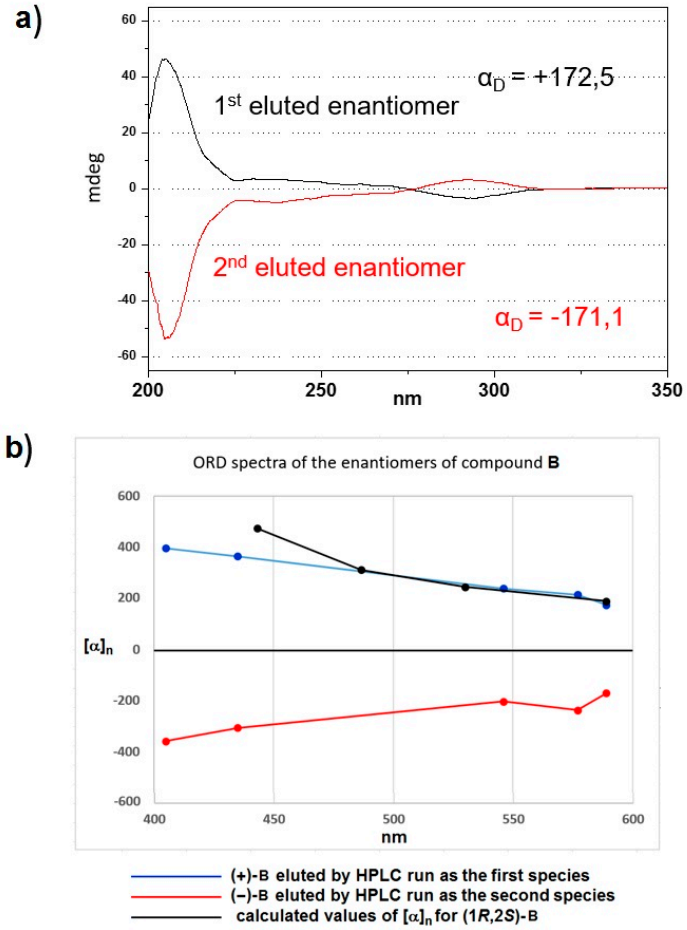

Figure 5. Experimental off-line ECD spectra of (+)/(−)-**B** purified enantiomers (**a**) and experimental and calculated optical rotatory dispersion (ORD)curves (**b**). The experimental ORD/ECD curves have been measured in hexane.

Table 1. Values of experimental and calculated optical rotation reported in the optical rotatory dispersion (ORD) spectra of Figure 5b.

Wavelength of $[\alpha]_n$ (nm)	$[\alpha]_n$ of (+)-B	$[\alpha]_n$ of (−)-B	$[\alpha]_n$ of (1*R*, 2*S*)-B
589	172	−171	186
577	212	−238	-
546	237	−204	-
530	-	-	242
487	-	-	309
443	-	-	473
435	363	−307	-
405	395	−359	-

2.3. Determination of Absolute Configuration by Density Functional Theory (DFT)/ORD Calculations

(1*R*, 2*S*)-**B** = *N*-((1*R*, 2*S*)-2-amino-1,2-diphenylethyl)-2-isopropylbenzenamine

In the perspective to attribute the absolute configuration to each of the enantiomers of compound **B** eluted by e-HPLC as well as the resolved peaks, the experimental optical rotatory dispersion (ORD) displayed by such eluted species has been compared to that assessed by calculation for just one of the enantiomers [27–31]. To this purpose, in the first step of the adopted procedure, the structural flexibility of **B** was analyzed through molecular modeling approach. The conformational search, performed on the (1*R*, 2*S*)-**B** stereoisomer and based on classical molecular mechanics calculations, suggested a wide flexibility of **B**, as summarized by the obtainment of 22 geometries found within a range of 3 kcal·mol^{-1} from the global minimum. However, after suitable refinement in two steps of these geometries and of their relevant energy stabilities at a higher level of theory (i.e., through HF and, next, DFT calculations, for details see the section 3), only two final conformations, endowed with an estimated overall Boltzmann Population (BP) amounting to about 78%, have been obtained. From such a couple of geometries, the relevant optical rotation values $[\alpha]_n$ at four different wavelengths n, in the range 443–589 nm have been assessed, again at the DFT level of theory. Thus, from such data, the final ORD spectrum relevant to the (1*R*, 2*S*)-**B** enantiomer could be simulated, which displayed an increasing trend of positive $[\alpha]_n$ values in answer to a progressive reduction of wavelength. The comparison of this computed ORD spectrum with the relevant experimental ones (see Figure 5b and Table 1) allowed us to attribute with reasonable reliability the (1*R*, 2*S*) configuration to the enantiomer of **B** that in the e-HPLC resolution was eluted as the first peak.

As a corollary to the DFT/ORD analysis, by comparing the ECD spectra of the diamine precursors and of the final catalysts (Figure 3 dotted and bold black traces for (+)-**B** and **1a**), and taking into account that the synthetic steps from the enantiopure diamine to the corresponding catalyst do not modify the stereochemistry of chiral carbons, it can be assumed that the absolute configuration of precursor has been maintained in the respective Ru-catalyst. Therefore, the (1*R*, 2*S*) configuration matches with Ru-catalyst **1a**.

2.4. Asymmetric Metathesis Transformations

The catalytic behaviour of enantiopure Ru-catalysts **1a** and **1b** was first evaluated in model asymmetric ring-closing metathesis (ARCM) reactions of prochiral trienes **5** and **6** (Scheme 2) and the results are summarized in Table 2. To ensure reproducibility, all reactions were performed at least in duplicate in the presence of each enantiomer. Since **1a** and **1b**, as expected, gave essentially the same selectivities while producing opposite enantiomers of **7** and **8**, for a better understanding of the results, only the ARCM reactions promoted by the enantiomer **1b** are reported in Table 2. For comparison, parallel ARCM reactions performed with catalysts **2** and **4** incorporating *anti* phenyl groups on the backbone were included in the table. Moreover, to put our results in a more general context, parallel reactions promoted by Collins's catalyst (Figure 1) were also added [15,16,32]. Indeed, this latter

represents the most enantioselective C_1-symmetric system which is structurally very similar to the aforementioned catalysts.

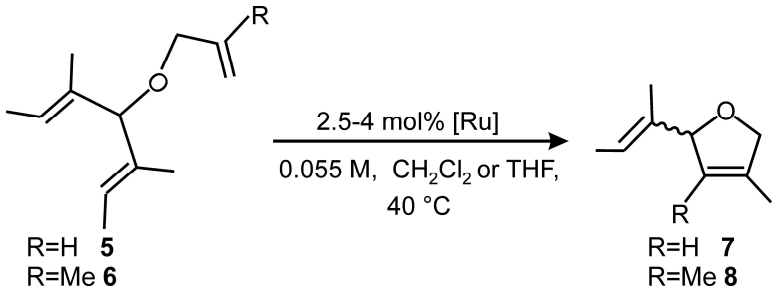

Scheme 2. Asymmetric ring-closing metathesis (ARCM) of trienes **5** and **6**.

Table 2. Asymmetric ring-closing metathesis of **5** and **6** with **1b**.

Entry [a]	Substrate	Catalyst (mol %)	Additive	Time (h)	Yield (%) [b]	ee % [c]
1	5	1b (2.5)	none	2	>98	37 (*R*) [1a:39(S)] [d]
2	5	1b (4.0)	NaI	2	46	44 (*R*)
3	5	1b (4.0)	NaI	16	57	44 (*R*)
4	5	1b (2.5)	none	2	>98	39 (*R*) (22 °C)
5	5	1b (2.5)	NaI	2	56	39 (*R*) (0 °C)
6 [e]	5	2 (2.5)	none	2	>98	18 (*S*)
7 [e]	5	2 (4.0)	NaI	2	>95	53 (*S*)
8 [e]	5	4 (2.5)	none	2	>98	33 (*S*)
9 [e]	5	4 (4.0)	NaI	2	>95	50 (*S*)
10 [f]	5	Collins (2.5)	none	2	>95	82 (*S*)
11 [f]	5	Collins (4.0)	NaI	2	>95	48 (*S*)
12	6	1b (2.5)	none	2	>98	14 (*S*)
13	6	1b (4.0)	NaI	3	-	-
14 [e]	6	2 (2.5)	none	2	>95	42 (*S*)
15 [e]	6	2 (4.0)	NaI	3	-	-
16 [e]	6	4 (2.5)	none	2	>95	25 (*R*)
17 [e]	6	4 (4.0)	NaI	3	-	-
18 [g]	6	Collins (2.5)	none	3	95	8 (*S*)

[a] Runs without additives were carried out in dry CH_2Cl_2, while runs with NaI were performed in dry tetrahydrofuran (THF); [b] yields based on ^{1}H nuclear magnetic resonance (NMR) analysis; [c] enantiomeric excesses determined by chiral gas chromatography (GC); [d] as a representative example, data in parentheses are for the same reaction performed with **1a**; [e] taken by ref. [25,26]; [f] ref. [15,16]; [g] ref. [32].

The enantioselective desymmetrization of triene **6** with catalyst **1b** proceeded almost quantitatively with a moderate enantiomeric excess (entry 1, Table 2), which is twice as high as the value reached in the same reaction promoted by analogous *anti* catalyst **2** (entry 6), and unexpectedly very close to that obtained with *anti* catalyst **4** (entry 8), differing for the nature of the *N*-substituent (methyl instead of cyclohexyl). The use of NaI as an additive to enhance enantioselectivity [12,13] (entry 2) led only to a slight improvement in the ee % value, along with a detrimental effect on catalyst activity. Prolonged reaction time did not have a significant enhancement in product yield and did not show any effect on enantioselectivity (entry 3). Very likely, the diiodide derivative is rather unstable and decomposed under the employed reaction conditions after a few hours. Lower temperatures did not lead to an improvement in the ee % values (entries 4 and 5); at 0 °C, a considerable decrease in the formation of cyclic product **7** was observed. Compared to Collins's catalyst, as previously observed for **2** and **4** [26], **1b** exhibited lower enantioselectivity, benefiting from the use of NaI, albeit to a minor extent (entries 10 and 11). This finding confirms that both the nature and the relative orientation of substituents on the backbone of C_1-symmetric NHCs may strongly influence catalyst enantioselectivity.

Regardless of the poor efficiency displayed by parent racemic catalyst **1** in the ring-closing metathesis of hindered diene substrates, we thought to investigate the catalytic behaviour of enatiopure **1b** in the challenging ARCM of **6** to form tetrasubstituted cycloolefin **8**. **1b** was found to successfully accomplish this difficult ring-closure, giving a lower value of ee % with respect to both **2** and **4** (entries 14 and 16), but slightly higher with respect to Collins's catalyst (entry 18). The opposite enantiomer was obtained, as also found in the ARCM promoted by *anti* catalyst **4**. Again, a close similarity of the catalytic behaviour of **1b** to that of **4**, presenting a small *N*-methyl group, rather than to that of **2**, having the same bulky *N*-cyclohexyl substituent, was observed. These results indicate that changing backbone configuration of NHC ligands bearing an encumbered *N*-cyclohexyl group (from **2** to **1b**) produces almost the same effect of varying bulkiness of *N*-alkyl substituents (from **2** to **4**) on the stereochemical outcome of the reaction. This suggests that the chiral environment created around the metal by this class of C_1-simmetric ligands may be strongly altered by the relative orientation of the substituents on the backbone, providing a further key element in the design of chiral NHC ligands. The addition of NaI to improve enantioselectivity inhibited the reaction completely, as already observed in the same ARCM transformations performed with **2** and **4** [26].

The catalytic behaviour of **1b** (and of its enantiomer **1a**) was then evaluated in another model asymmetric metathesis transformation, the AROCM of cis-5-norbornene-endo-2,3-dicarboxylic anhydride (**10**) with styrene (Scheme 3), and subsequently compared to those of **2** and **4** (Table 3).

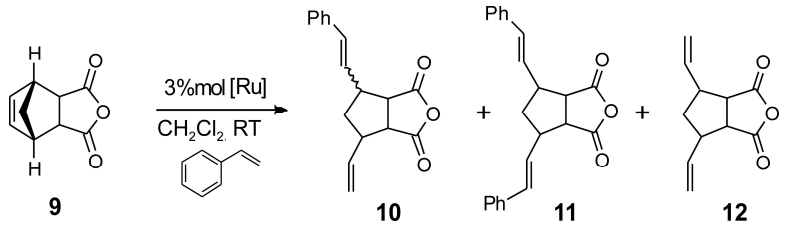

Scheme 3. Asymmetric ring-opening cross-metathesis (AROCM) of anhydride **9** with styrene.

Table 3. Asymmetric ring-opening cross-metathesis of **9** with styrene in the presence of **1b**.

Entry [a]	Catalyst	10 Yield [b]	11 Yield [b]	12 Yield [b]	ee % (10) [c]
1	1b	70	1	29	15
2 [d]	2	45	10	10	32
3 [d]	4	20	5	11	29

[a] [9] = 0.07 M in CH_2Cl_2, 10 eq. styrene, 2 h; [b] isolated yield; [c] enantiomeric excess determined by chiral HPLC; [d] taken by ref. [26].

After reaction of anhydride **9** with 10 equivalents of styrene in CH_2Cl_2 for 2 h, the desired product **9** was obtained in high isolated yield but low enantiomeric excess (entry 1, Table 3). As already found for **2** and **4** (entries 2 and 3), the formation of side products **11** and **12** was observed [26,33]. Also in this case, only stilbene deriving from the cross-metathesis of styrene was detected, as well as only the products showing trans stereochemistry were detected [26,33]. Interestingly, although the introduction of *syn* backbone in the architecture of the NHC ligand resulted in a decreased enantioselectivity with respect to catalysts **2** and **4** with *anti* backbone, the distribution of products seemed to be affected by this NHC structure modification. Indeed, an increased yield in the desired product **10** was achieved, and a significant amount of side-product **12** with respect to **11** was obtained, suggesting that the key steps of the reaction might involve propagation via a ruthenium methylidene species, as generally observed for catalysts characterized by unsymmetrical *N*-alkyl/*N*-aryl NHC ligands [34,35].

3. Materials and Methods

HPLC gradient grade solvents were obtained from Sigma-Aldrich (St. Louis, MO, USA). Chiral columns were from Chiral Technologies Europe (Illkirch, France). All reagents were purchased from Sigma Aldrich Company or TCI Chemicals. Reactions involving organometallic compounds were performed under nitrogen using standard Schlenk and glove box techniques. Solvents were dried and distilled before use. Deuterated solvents were degassed under a N_2 flow and stored over activated 4 Å molecular sieves. Flash column chromatography of organic compounds were performed using silica gel 60 (230–400 mesh) from Sigma Aldrich Company and flash column chromatography of ruthenium complexes were performed, under N_2 flow, using silica gel 60 (230–400 mesh) from TSI Cambridge. Analytical thin-layer chromatography (TLC) was performed using silica gel 60 F254 precoated plates with a fluorescent indicator. The visualization was performed using UV-light. Optical activity for enantiomers of C and D was determined using a JASCO P2000 polarimeter. Enantiomeric excesses of **7**, **8** and **10** were determined by chiral GC (Supelco βDEX 120, 30 m × 0.25 mm) or by chiral HPLC (JASCO MD-4015 Photo diode array detector, PU4180 RMPLC Pump) and were compared to racemic samples.

3.1. Enantioselective Chromatography and Chiro-Optical Characterization

Analytical liquid chromatography was performed on a Jasco HPLC system equipped with a PU-980 HPLC pump, a 20 μL loop injector (Rheodyne model 7725i), a 975 series UV detector and a 995-CD series detector. Chromatographic data were collected and processed with Jasco Borwin software (Version 1.50, Jasco Europe, Italy). Semi-preparative liquid chromatography was performed on a Waters chromatograph (Waters, Milford, MA, USA) equipped with a Rheodyne model 7012, 500 μL loop injector and a spectrophotometer UV SpectraMonitor 4100 (Waters, Milford, MA, USA).

The enantiomers of **B** were resolved by using the Chiralpak IA column (250 × 10 mm ID, 5 μm), *n*-hexane/isopropanol 90/10 as eluent (flow rate 3.0 mL/min, T: 25 °C and UV detection at 300 nm). The sample was dissolved in hexane/isopropanol/dichloromethane 70/10/20 (*c*: 50 mg/mL); each injection was of 100 μL (process yield 70%). The enantiomeric excess of each collected enantiomer was determined by analytical HPLC with the Chiralpak IA column (250 × 4.6 mm ID, 5 μm) under the same elution conditions with a flow rate of 1.0 mL/min and UV/CD detections at 254 and 300 nm respectively.

The off-line ECD spectra of hexane solutions of chromatographically resolved (+)-**B** and (−)-**B** ($c = 3 \times 10^{-4}$ M) and the enantiopure catalysts **1a** and **1b** were recorded with a J710 UV-CD Jasco spectrometer. Specific optical rotations of hexane solutions of (+)-**B** and (−)-**B** (*c* = 0.097% and 0.103%) were measured with a polarimeter P-1020 Jasco (Jasco Europe, Italy) at 25 °C at 589, 577, 546, 435, 405 and 365 nm. HPLC gradient grade solvents were obtained from Sigma-Aldrich (St. Louis, MO).

*3.2. Simulation of the ORD Spectrum of the (1R, 2S)-**B** Enantiomer.*

Molecular modeling calculations carried out on the structure of the (1*R*, 2*S*)-**B** enantiomer and concerning conformational search and optimization of the so-obtained geometries, were performed by using the computer program SPARTAN 10v1.1.0 (Wavefunction Inc., 18401 Von Karman Avenue, Suite 370, Irvine, CA, USA). The conformational search was performed by molecular mechanic calculations based on the Merck molecular force field (MMFF), according to the systematic algorithm implemented in SPARTAN. All rotatable bonds were varied. Maximum energy gap from the lowest energy geometry for kept conformations was 40 kJ·mol^{-1}; criterion adopted in the analysis of similarity to define conformers as duplicates was $R^2 \geq 0.9$. Such analysis supplied a total of 27 conformations, 22 of which by an energy window of 3 kcal·mol^{-1}. All the geometries were further optimized at the HF/STO-3G level of theory, which afforded 15 conformations within an energy window of 3 kcal·mol^{-1}. Among these latter, the seven more stable conformations from the global minimum (hereafter denoted with the symbol C_n, with *n* varying between 1 and 7), which covered a range of Boltzmann distribution

amounting overall to 79.1%, were, in turn, further optimized by minimizing their energy stability at the level of theory B3LYP/6-31G*. In all such calculations, the effect of the hexane as the solvent, by simulating its presence according to the SM8 model implemented in SPARTAN, was taken into account. The found relative difference in energy of the conformers $C_{2–7}$ with respect to C_1 were: C_2 = 0.11, C_3 = 0.41, C_4 = 2.04, C_5 = 3.39, C_6 = 4.66, C_7 = 5.03 kcal·mol^{-1}. The corresponding percentages of Boltzmann distributions were C_1 = 42.3, C_2 = 35.1, C_3 = 21.1, C_4 = 1.4, C_5 = 0.1, C_6 = 0.0 and C_7 = 0.0, respectively. Due to the high level of geometric and energetic similarity existing between the two conformers found to be the most stable, C_1 and C_2 (i.e., the ones differing by only 0.11 kcal·mol^{-1}), they were clustered in a single global minimum geometry, denoted as $C_{1,2}$. Thus, among the seven initial conformations optimized by means of the B3LYP method, just the final two geometries $C_{1,2}$ and C_3 were endowed with a significant amount of Boltzmann distribution (65.1% and 32.5%, respectively); they were therefore employed in the next step of the modelling, focused on assessing the relevant optical rotatory dispersion (ORD) spectra of (1*R*, 2*S*)-**B**. Conformations $C_{1,2}$ and C_3 were than subjected to assessment of optical rotation values $[\alpha]_n$ at four different wavelengths n, in the range 443–589 nm, which were carried out by using the BLYP method with the TZ2P large core basis set, as implemented in the Amsterdam Density Functional (ADF) package v. 2007.01. The couples of $[\alpha]_n$ values obtained at each wavelength from the geometries of $C_{1,2}$ and C_3 were weighted according to the Boltzmann distributions calculated for the related conformations, and then merged onto each other, thus affording (1*R*, 2*S*)-**B** the following final optical rotation values: $[\alpha]_{443}$ = 473 nm; $[\alpha]_{487}$ = 309 nm; $[\alpha]_{530}$ = 242 nm; $[\alpha]_{589}$ = 186 nm.

3.3. Catalytic Tests

ARCM of **5** and **6** without additive (Scheme 2) were carried out by adding the catalyst (0.0028 mmol, 0.025 eq.) to a 2 mL solution of the prochiral triene (1 eq., 0.055 M) in dry CD_2Cl_2. The flask was stirred a 40 °C for two hours for **6** and for three hours for **7**. Yields were determined via NMR spectroscopy of the crude product. The reaction mixture was filtered on neutral alumina and injected into the GC system without further purifications.

ARCM of **5** and **6** with additive (Scheme 2) were implemented by adding NaI (0.055 mmol, 1 eq.) to a 1 mL THF-d8 solution of the catalyst (0.0022 mmol, 0.04 eq.). The reaction mixture was stirred at room temperature for one hour. After that, **6** or **7** (0.055 mmol, 1 eq.) was added. Then, the flask was stirred a 40 °C for two hours for **6** and three hours for **7**. Yields were determined via NMR spectroscopy of the crude product. The reaction mixture was filtered on neutral alumina and injected into the GC system without further purifications.

AROCM of **9** with styrene (Scheme 3) in glove box, 9 (0.43 mol, 1 eq.) and styrene (4.3 mmol, 10 eq.) were simultaneously added to 7.5 mL of CH_2Cl_2 solution of the catalyst (0.013 mmol, 0.03 eq.). The flask was stirred at room temperature for three hours. The reaction mixture was then concentrated and purified via column chromatography (petroleum ether:diethyl ether, 1:1) to afford the product as a transparent oil. About 1 mg of the product was dissolved in 1 mL of 2-propanol (HPLC-grade purity), filtered using a syringe filter and then injected into the HPLC system.

4. Conclusions

In summary, we reported the synthesis of ruthenium metathesis catalysts **1a** and **1b** possessing enantiopure C_1-symmetric *N*-Heterocyclic carbenes (NHC) ligands with *syn* phenyl groups on the backbone and *N*-cyclohexyl/*N*-2-isopropylphenyl substituents. This type of NHC architecture is unexplored in ruthenium-catalyzed asymmetric metathesis to date. Enantiomeric catalysts **1a** and **1b** were evaluated in model asymmetric ring-closing metathesis (ARCM) and asymmetric ring-opening cross-metathesis (AROCM) reactions, displaying moderate enantioselectivities, and compared to the corresponding catalysts with an *anti* NHC backbone configuration. The nature of the stereochemical relationship of NHC backbone substituents in C_1-symmetric ligands was found to play a role in addressing catalyst activity and selectivity. Therefore, although enantioselectivity levels are still far

from those of other similar catalysts described in the literature, the preliminary results reported herein encourage the development of new C_1-symmetric NHCs with a *syn* backbone for the rational design of more stereoselective ruthenium metathesis catalysts.

Supplementary Materials: Representative NMR spectra (Figures S1–S4) and chromatograms (Figures S5–S10) are available online at www.mdpi.com/2073-4344/6/11/177/s1.

Acknowledgments: Financial supports from the Ministero dell'Università e della Ricerca Scientifica e Tecnologica and from Sapienza University of Rome are gratefully acknowledged.

Author Contributions: A.C. and F.G. conceived and designed the experiments; V.P. performed the synthesis and NMR spectroscopic characterization; G.D.S. contributed analysis tools; S.M. performed the chromatographic and spectroscopic experiments; M.P. performed the computational study; A.C. and F.G. analyzed the data and wrote the paper.

Conflicts of Interest: The authors declare no conflict of interest.

References

1. Hopkinson, M.N.; Richter, C.; Schedler, M.; Glorius, F. An overview of *N*-Heterocyclic carbenes. *Nature* **2014**, *510*, 485–496. [CrossRef] [PubMed]
2. Nolan, S.P. *N-Heterocyclic Carbenes: Effective Tools for Organometallic Synthesis*; Wiley-VCH: Weinheim, Germany, 2014.
3. Cazin, C.S.J. *N-Heterocyclic Carbenes in Transition Metal Catalysis and Organocatalysis*; Springer: Dordrecht, The Netherlands, 2011.
4. Fevre, M.; Pinaud, J.; Gnanou, Y.; Vignolle, J.; Taton, D. *N*-Heterocyclic carbenes (NHCs) as organocatalysts and structural components in metal-free polymer synthesis. *Chem. Soc. Rev.* **2013**, *42*, 2142–2172. [CrossRef] [PubMed]
5. César, V.; Bellemin-Laponnaz, S.; Gade, L.H. Chiral *N*-heterocyclic carbenes as stereodirecting ligands in asymmetric catalysis. *Chem. Soc. Rev.* **2004**, *33*, 619–636. [CrossRef] [PubMed]
6. Wang, F.; Liu, L.-J.; Wang, W.; Li, S.; Shi, M. Chiral NHC–metal-based asymmetric catalysis. *Coord. Chem. Rev.* **2012**, *256*, 804–853. [CrossRef]
7. Vougioukalakis, G.C.; Grubbs, R.H. Ruthenium-Based Heterocyclic Carbene-Coordinated Olefin Metathesis Catalysts. *Chem. Rev.* **2010**, *110*, 1746–1787. [CrossRef] [PubMed]
8. Samojlowicz, C.; Bieniek, M.; Grela, K. Ruthenium-Based Olefin Metathesis Catalysts Bearing *N*-Heterocyclic Carbene Ligands. *Chem. Rev.* **2009**, *109*, 3708–3742. [CrossRef] [PubMed]
9. Tornatzky, J.; Kannenberg, A.; Blechert, S. New catalysts with unsymmetrical *N*-heterocyclic carbene ligands. *Dalton Trans.* **2012**, *41*, 8215–8225. [CrossRef] [PubMed]
10. Kress, S.; Blechert, S. Asymmetric catalysts for stereocontrolled olefin metathesis reactions. *Chem. Soc. Rev.* **2012**, *41*, 4389–4408. [CrossRef] [PubMed]
11. Paradiso, V.; Costabile, C.; Grisi, F. NHC backbone configuration in ruthenium-catalyzed olefin metathesis. *Molecules* **2016**, *21*, E117. [CrossRef] [PubMed]
12. Seiders, T.J.; Ward, D.W.; Grubbs, R.H. Enantioselective Ruthenium-Catalyzed Ring-Closing Metathesis. *Org. Lett.* **2001**, *3*, 3225–3228. [CrossRef] [PubMed]
13. Funk, T.W.; Berlin, J.M.; Grubbs, R.H. Highly Active Chiral Ruthenium Catalysts for Asymmetric Ring-Closing Olefin Metathesis. *J. Am. Chem. Soc.* **2006**, *128*, 1840–1846. [CrossRef] [PubMed]
14. Berlin, J.M.; Goldberg, S.D.; Grubbs, R.H. Highly Active Chiral Ruthenium Catalysts for Asymmetric Cross- and Ring-Opening Cross-Metathesis. *Angew. Chem. Int. Ed.* **2006**, *45*, 7591–7595. [CrossRef] [PubMed]
15. Fournier, P.; Collins, S.K. A Highly Active Chiral Ruthenium-Based Catalyst for Enantioselective Olefin Metathesis. *Organometallics* **2007**, *26*, 2945–2949. [CrossRef]
16. Fournier, P.; Savoie, J.; Stenne, B.; Bédard, M.; Grandbois, A.; Collins, S.K. Mechanistically Inspired Catalysts for Enantioselective Desymmetrizations by Olefin Metathesis. *Chem. Eur. J.* **2008**, *14*, 8690–8695. [CrossRef] [PubMed]
17. Grandbois, A.; Collins, S.K. Enantioselective Synthesis of [7] Helicene: Dramatic Effects of Olefin Additives and Aromatic Solvents in Asymmetric Olefin Metathesis. *Chem. Eur. J.* **2008**, *14*, 9323–9329. [CrossRef] [PubMed]
18. Savoie, T.; Stenne, B.; Collins, S.K. Improved Chiral Olefin Metathesis Catalysts: Increasing the Thermal and Solution Stability via Modification of a C_1-Symmetrical *N*-Heterocyclic Carbene Ligand. *Adv. Synth. Catal.* **2009**, *351*, 1826–1832. [CrossRef]

19. Van Veldhuizen, J.J.; Garber, S.B.; Kingsbury, J.S.; Hoveyda, A.H. A Recyclable Chiral Ru Catalyst for Enantioselective Olefin Metathesis. Efficient Catalytic Asymmetric Ring-Opening/Cross Metathesis in Air. *J. Am. Chem. Soc.* **2002**, *124*, 4954–4955. [CrossRef] [PubMed]
20. Gillingham, D.G.; Kataoka, K.; Garber, S.B.; Hoveyda, A.H. Efficient Enantioselective Synthesis of Functionalized Tetrahydropyrans by Ru-Catalyzed Asymmetric Ring-Opening Metathesis/Cross-Metathesis (AROM/CM). *J. Am. Chem. Soc.* **2004**, *126*, 12288–12290. [CrossRef] [PubMed]
21. Van Veldhuizen, J.J.; Campbell, J.E.; Giudici, R.E.; Hoveyda, A.H. A Readily Available Chiral Ag-Based *N*-Heterocyclic Carbene Complex for Use in Efficient and Highly Enantioselective Ru-Catalyzed Olefin Metathesis and Cu-Catalyzed Allylic Alkylation Reactions. *J. Am. Chem. Soc.* **2005**, *127*, 6877–6882. [CrossRef] [PubMed]
22. Giudici, R.E.; Hoveyda, A.H. Directed Catalytic Asymmetric Olefin Metathesis. Selectivity Control by Enoate and Ynoate Groups in Ru-Catalyzed Asymmetric Ring-Opening/Cross-Metathesis. *J. Am. Chem. Soc.* **2007**, *129*, 3824–3825. [CrossRef] [PubMed]
23. Tiede, S.; Berger, A.; Schlesiger, D.; Rost, D.; Lühl, A.; Blechert, S. Highly Active Chiral Ruthenium-Based Metathesis Catalysts through a Monosubstitution in the *N*-Heterocyclic Carbene. *Angew. Chem. Int. Ed.* **2010**, *49*, 3972–3975. [CrossRef] [PubMed]
24. Kannenberg, A.; Rost, D.; Eibauer, S.; Tiede, S.; Blechert, S. A Novel Ligand for the Enantioselective Ruthenium-Catalyzed Olefin Metathesis. *Angew. Chem. Int. Ed.* **2011**, *50*, 3299–3302. [CrossRef] [PubMed]
25. Paradiso, V.; Bertolasi, V.; Grisi, F. Novel Olefin Metathesis Ruthenium Catalysts Bearing Backbone-Substituted Unsymmetrical NHC Ligands. *Organometallics* **2014**, *33*, 5932–5935. [CrossRef]
26. Paradiso, V.; Bertolasi, V.; Costabile, C.; Grisi, F. Ruthenium Olefin Metathesis Catalysts Featuring Unsymmetrical *N*-Heterocyclic Carbenes. *Dalton Trans.* **2016**, *45*, 561–571. [CrossRef] [PubMed]
27. Stephens, P.J.; Devlin, F.J.; Gasparrini, F.; Ciogli, A.; Spinelli, D.; Cosimelli, B. Determination of the absolute configuration of a chiral oxadiazol-3-one calcium channel blocker, resolved using chiral chromatography, via concerted density functional theory calculations of its vibrational circular dichroism, electronic circular dichroism, and optical rotation. *J. Org. Chem.* **2007**, *72*, 4707–4715. [PubMed]
28. Ioan, P.; Ciogli, A.; Sirci, F.; Budriesi, R.; Cosimelli, B.; Pierini, M.; Severi, E.; Chiarini, A.; Cruciani, G.; Gasparrini, F.; Spinelli, D.; Carosati, E. Absolute configuration and biological profile of two thiazinooxadiazol-3-ones with L-type calcium channel activity: A study of the structural effects. *Org. Biomol. Chem.* **2012**, *10*, 8994–9003. [CrossRef] [PubMed]
29. Giorgio, E.; Viglione, R.G.; Zanasi, R.; Rosini, C. Ab Initio Calculation of Optical Rotatory Dispersion (ORD) Curves: A Simple and Reliable Approach to the Assignment of the Molecular Absolute Configuration. *J. Am. Chem. Soc.* **2004**, *126*, 12968–12976. [CrossRef] [PubMed]
30. Rotili, D.; Samuele, A.; Tarantino, D.; Ragno, R.; Musmuca, I.; Ballante, F.; Botta, G.; Morera, L.; Pierini, M.; Cirilli, R.; et al. 2-(Alkyl/aryl)amino-6-benzylpyrimidin-4(3*H*)-ones as inhibitors of wild-type and mutant HIV-1: Enantioselectivity studies. *J. Med. Chem.* **2012**, *55*, 3558–3562. [CrossRef] [PubMed]
31. Vaghi, L.; Benincori, T.; Cirilli, R.; Alberico, E.; Mussini, P.R.; Pierini, M.; Pilati, T.; Rizzo, S.; Sannicolò, F. Ph-tetraMe-bithienine, the first member of the class of chiral heterophosphepines: Synthesis, electronic and steric properties, metal complexes and catalytic activity. *Eur. J. Org. Chem.* **2013**, *2013*, 8174–8184. [CrossRef]
32. Stenne, B.; Timperio, J.; Savoie, J.; Dudding, T.; Collins, S.K. Desymmetrizations Forming Tetrasubstituted Olefins Using Enantioselective Olefin Metathesis. *Org. Lett.* **2010**, *12*, 2032–2035. [CrossRef] [PubMed]
33. Thomas, R.M.; Grubbs, R.H. Mechanistic Studies of Enantioselective *N*-aryl, *N*-alkyl NHC Ruthenium Metathesis Catalysts in Asymmetric Ring-Opening Cross-Metathesis. *Chem. N. Z.* **2011**, *75*, 65–71.
34. Stewart, I.C.; Keitz, B.K.; Kuhn, K.M.; Thomas, R.M.; Grubbs, R.H. Nonproductive events in ring-closing metathesis using ruthenium catalysts. *J. Am. Chem. Soc.* **2010**, *132*, 8534–8535. [CrossRef] [PubMed]
35. Keitz, B.K.; Grubbs, R.H. Probing the Origin of Degenerate Metathesis Selectivity via Characterization and Dynamics of Ruthenacyclobutanes Containing Variable NHCs. *J. Am. Chem. Soc.* **2011**, *133*, 16277–16284. [CrossRef] [PubMed]